MODELING WINTER CLOUDS WITH THE MM5 MODEL

Roy Rasmussen, Jon Reisner and Roelof Bruintjes
National Center for Atmospheric Research – Research Applications Program
Boulder, Colorado

1. INTRODUCTION

Winter storms have a major impact on human activity, from transportation to agriculture. The aviation industry is particularly impacted by a variety of winter phenomena including icing of aircraft on the ground, in-flight aircraft icing, and reduced ceiling and visibility. Improved forecasts of these winter phenomena would clearly benefit safety and capacity at impacted airports.

The winter weather problem has been the subject of numerous field programs. Most, however, have focussed on oceanic winter storms (GALE, ERICA, CYCLES and CASP for example). A few recent field programs have focussed on continental winter storms (STORM-FEST, WISP for example). The Winter Icing and Storms Project (WISP) focussed its efforts on winter storms occurring in eastern Colorado. A description of WISP, including preliminary scientific findings from two major field efforts in 1990 and 1991 was given by Rasmussen et al. (1992). The main goals of WISP are to improve forecasts of aircraft icing and to improve our understanding of the production and depletion of supercooled liquid water (SLW).

Aircraft ice up when they encounter supercooled liquid water in the atmosphere. Current operational models at the U.S. National Meteorological Center do not explictly predict SLW, requiring the use of proxy variables such as temperature and relative humidity to forecast regions of aircraft icing. An explicit prediction of cloud water is clearly desired, however. For this reason, recent research has concentrated on efforts to incorporate microphysical parameterizations into numerical models to explicitly predict regions of water and ice and the interaction between both species. NMC has implemented a parameterization for cloud water (Q_c) and cloud ice (Q_i) (Zhao et al., 1991) into an experimental version (40 km horizontal resolution) of the Eta model (Black and Messinger, 1989). However, at a horizontal resolution of 40 km it is currently uncertain if the model will resolve regions of cloud liquid water content on scales associated with mesoscale precipitation phenomena and snow bands in winter storms. In addition, it is well known that microphysical parameterizations that predict Q_c are relatively crude and can produce results that do not conform to reality. Therefore, more research is needed to evaluate and validate the accuracy of the current parameterizations that predict Q_c on scales from 10 to 100 km.

As a result, recent and current research at the Research Applications Program (NCAR) with regard to the implementation and evaluation of microphysical parameterizations has concentrated on two goals: 1) to develop and upgrade microphysical parameterizations for use in numerical models which predict icing potential on a national scale; and 2) to evaluate and validate these parameterizations with data obtained from WISP field programs. Because the previous WISP field programs were all conducted along the Front Range of Colorado, the evaluation and validation efforts concentrated on this region. To date, three field studies have been conducted with the first occurring from 1 February to 31 March 1990 (WISP90), the second occurring from 15 January to 5 April 1991 (WISP91), and the third occurring from 25 January to 25 March 1994 (WISP94). During the coarse of the three field studies, extensive microphysical measurements were made in upslope storms of varying types (e.g., Table 1 in Rasmussen et al 1992).

2. OVERVIEW OF THE MICROPHYSICAL PARAMETERIZATION

The mesoscale model used in the simulations described below is a nonhydrostatic extension (hereafter referred to as MM5) of the hydrostatic model (previously referred to as MM4) presented by Anthes and Warner (1978). MM5 can accommodate four-dimensional data assimilation, multi-nested domains, and various physical parameterizations (Grell et al. 1994). MM5 can be initialized with data obtained from an analysis package that incorporates raw upper-air, surface data, and/or data from other numerical weather prediction models (Manning and Haagenson 1994). Raw data can also be reformatted to provide lateral boundary conditions for a particular nest at later times into the simulation.

During a simulation, any one of five microphysical options listed below can be activated:

1. Bulk warm rain model with mixing ratios of water vapor (Q_v), Q_c, and rain (Q_r) predicted (Hsie et al. 1984).

2. Bulk cold rain model with mixing ratios of cloud ice (Q_i) or Q_c (for $T > 0°C$) in one predictive field and Q_s or Q_r (for $T > 0°C$) in another predictive field (Dudhia 1989).

3. Bulk cold rain model with mixing ratios of Q_i, Q_s, Q_c, and Q_r predicted.

4. Bulk cold rain model with the mixing ratios of Q_i, Q_s, graupel (Q_g), Q_c, Q_r, and number concentration of Q_i (N_i) predicted.

5. Bulk cold rain model with the mixing ratios of Q_i, Q_s, Q_g, Q_c, Q_r, N_i, number concentration of Q_s (N_s), and number concentration of Q_g (N_g) predicted.

Options 3, 4 and 5 were developed by the authors. A detailed description of option 5 is

presented in Appendix A. Figure 1 provides an overview of all the different interactive microphysical processes that are included in option 5.

The main difference between options 2 and 3 is the addition of two additional arrays to allow the co-existence of cloud ice and cloud water at temperatures below freezing, and to allow rain water and snow to co-exist below freezing. In addition, options 3 and 4 also includes a parameterization for the melting of snow, evaporation of melting snow, and the heterogeneous freezing of cloud water. In option 3, the slope intercept in the Marshall-Palmer Distribution for snow is a function of the mixing ratio of snow (Appendix A).

The differences between option 3 and option 4 are more significant. One of the major differences between the two options is the parameterizations used in the conversion of Q_i into Q_s. In option 3 the conversion process follows that suggested by Kessler (1969); whereas, in option 4 a more complex three step procedure developed by Murakami (1990) and Ikawa and Saito (1991) is used. One of the many benefits of the parameterization in option 4 is that the aggregation of ice crystals is more realistically simulated.

By explicitly forecasting N_s and N_g, Option 5 eliminates the need for prescribing N_{os} and N_{og} by explicitly predicting N_s and N_g. However, in addition to the computational cost involved in advecting two more variables, complex and hence costly parameterizations for the sources and sinks of N_s and N_g had to be incorporated. Even though option 5 typically requires 45/25 percent more computer resources than option 3/4, option 5 usually produces a SLW field which agrees better with the observed data than is produced by simulations employing either options 3 or 4.

3. INTERCOMPARISON TO WISP CASE STUDIES

In the previous version of the microphysical parameterization only the mixing ratios for the different water species in the model were predicted and the number concentration of the ice species were prescribed. This was changed in the upgraded version of the parameterization. The number concentrations for ice, snow and graupel are now also explicitly predicted in Option 5. The reason we added predictive equations for ice species number concentration was because cloud water was depleted too fast compared to observations from WISP cases when a fixed number concentration was prescribed (described below). This also provided a more realistic picture of what happens in the atmosphere where concentrations of ice, snow and graupel can change substantially depending on different environmental conditions.

In order to test the performance of the parameterization and examine the explicit prediction of supercooled liquid water (SLW), numerical simulations were conducted for two different WISP cases representing different types of storms. These were: 1) an anticyclonic storm (13-

15 February 1990, Rasmussen et al. (1995)); and 2) a deep cyclonic storm (5-7 March 1990). The simulations were conducted using four different domains with different horizontal resolutions of 60 km, 20 km, 6.7 km, and 2.2 km. The 20 km domain was run concurrently with the 60 km domain, whereas the 6.7 and 2.2 km domains were run in a one-way nest mode. Initial and boundary data for the 60 km domain were supplied from the National Meteorological Center's (NMC) archived forecast model fields. The results from the simulations were compared to data obtained from the WISP 1990 field program.

Comparison between the model results and the observations revealed that riming and depositional growth of snow and/or graupel were depleting SLW too rapidly when the number concentrations of the ice species were fixed. Specifically, specifying a constant $N_{o,s}$ resulted in unrealistically high depletion of cloud water through depositional and riming of Q_s than observed. Specifying $N_{o,s}$ as a function of Q_s reduced this tendency. Best comparison to observations were found when the number concentrations of the ice species were explicitly predicted. In this case, both riming and depositional growth were limited and the simulated microphysical fields agreed better with the observations.

4. ACKNOWLEDGEMENTS

This research is sponsored by the National Science Foundation through an Interagency Agreement in response to the requirements and funding by the Federal Aviation Administration's Aviation Weather Development Program. The views expressed are those of the authors and do not necessarily represent the official policy or position of the U.S. Government. The authors are grateful to Carol Makowski for typing this manuscript.

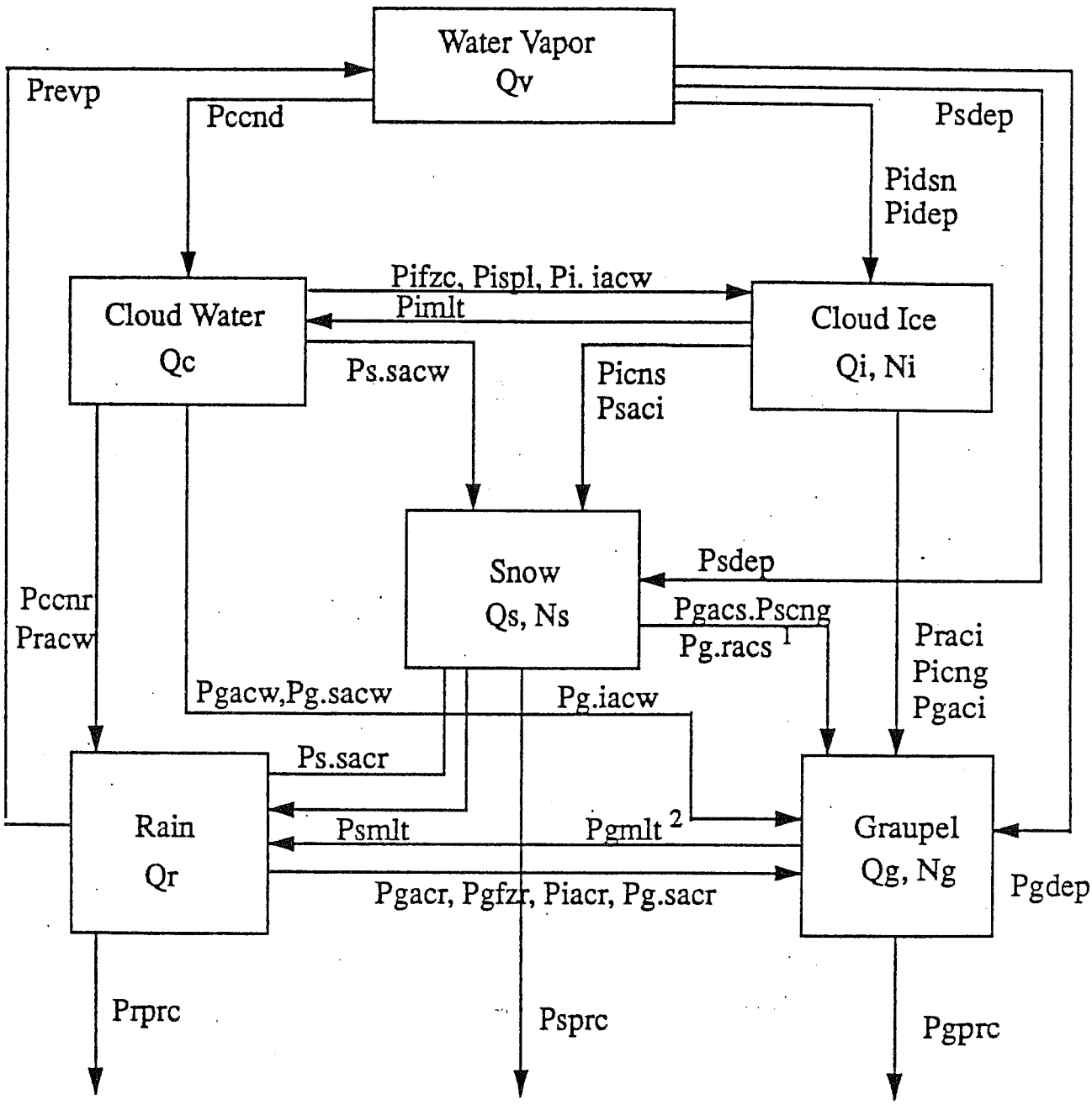
Cloud Microphysical Processes
Water Vapor
Qv
Prevp
Pccnd
Psdep
Pidsn
Pidep
Pifzc, Pispl, Pi. iacw
Pimlt
Cloud Water
Qc
Cloud Ice
Qi, Ni
Ps.sacw
Picns
Psaci
Snow
Qs, Ns
Psdep
Pccnr
Pracw
Pgacs.Pscng
Pg.racs 1
Praci
Picng
Pgaci
Pgacw,Pg.sacw
Pg.iacw
Ps.sacr
Rain
Qr
Psmlt
Pgmlt 2
Graupel
Qg, Ng
Pgacr, Pgfzr, Piacr, Pg.sacr
Pgdep
Prprc
Psprc
Pgprc

Figure 1

5. REFERENCES

Anthes, R.A., E.-Y. Hsie, and Y-H. Kou, 1987: Description of the Penn State/NCAR Mesoscale Model Version 4 (MM4). NCAR Technical Note NCAR/TN-282+STR, 66pp.

Bigg, E.K., 1953: The supercooling of water. *Proc., Phys. Soc.,* **B66, 688**, 157–162.

Black, T.L., and F. Mesinger, 1989: Forecast performance of NMC's eta coordinate regional model. Preprints, *12th Conf. on Wea. Anal. and Forecasting*, Monterey, CA, Amer. Meteor. Soc., 551-555.

Dudhia, J., 1989: Numerical study of convection observed during the winter monsoon experiment using a mesoscale two-dimensional model *J. Atmos. Sci.*, **46**, 3077-3107.

Fletcher, N.H., 1962: *The Physics of Rainclouds*, Cambridge University Press.

Grell, G. A., J. Dudhia, and D. R. Stauffer, 1994: *A description of the Fifth-Generation Penn State/NCAR Mesoscale Model (MM5).* NCAR/TN-398+IA, National Center for Atmospheric Research, CO, 107 pp.

Hallett, J. and S.C. Mossop, 1974: Production of secondary ice particles during the riming process. *Nature*, **249**, 26–28.

Hsie, E.-Y., R.A. Anthes, and D. Keyser, 1984: Numerical simulation of frontogenesis in a moist atmosphere. *J. Atmos. Sci.*, **41**, 2581–2594.

Ikawa, M., and K. Saito, 1991: Description of a nonhydrostatic model developed at the forecast research department of the MRI. Technical Reports of the Meteorological Research Institute, No. 28.

Kessler, E., 1969: On the distribution and continuity of water substance in atmospheric circulations. *Meteor. Monogr. No.*, **10**, Amer. Meteor. Soc.

Koenig, L.R., 1971: Numerical modeling of ice deposition. *J. Atmos. Sci.*, **28**, 226–237.

Lin, Y.-L., R.D. Farley, and H.D. Orville, 1983: Bulk parameterization of the snow field in a cloud model. *J. Climate Appl. Meteor.*, **22**, 1065–1092.

Locatelli, J.D., and P.V. Hobbs, 1974: Fallspeeds and masses of solid precipitation particles. *J. Geophys. Res.*, **79**, 2185–2197.

Manning, K. W., and P. L. Haagenson, 1994: *Data ingest and objective analysis for the*

PSU/NCAR modeling system: Programs **DATAGRID** *and* **RAWINS.** NCAR/TN-376+IA, National Center for Atmospheric Research, CO, 209 pp.

Murakami, M., 1990: Numerical modeling of dynamical and microphysical evolution of an isolated convective cloud – the 19 July 1981 CCOPE cloud. *J. Meteorol. Soc.*, **68**, 107–128.

Pasarelli, R.E., 1978: Theoretical and observational study of snow-size spectra and snowflake aggregation efficiencies. *J. Atmos. Res.*, **35**, 882–889.

Pruppacher, H.R. and Klett, J.D., 1980: *Microphysics of Cloud and Precipitation*, D. Reidel Publishing Company, 714 pp.

Rasmussen, R.M, B.C. Bernstein, M. Murakami, G. Stossmeister, J.M. Reisner and B. Stankov, 1995: The 1990 Valentine's Day arctic outbreak, Part I: Mesoscale and microscale structure and evolution of the Colorado Front Range shallow upslope cloud. Accepted for publication. *J. Appl. Meteor.*

Rasmussen, R.M., M. Politovich, J. Marwitz, W. Sand, J. McGinley, J. Smart, R. Pielke, S. Rutledge, D. Wesley, G. Stossmeister, B. Bernstein, K. Elmore, N. Powell, E. Westwater, B. Stankov and D. Burrows, 1992: Winter Icing and Storms Project (WISP). *Bull. Amer. Meteorol. Soc.*, **73**, 951–974.

Rutledge, S.A. and P.V. Hobbs, 1983: The mesoscale and microscale structure and organization of clouds and precipitation in midlatitude cyclones. Part VIII: a model for the "seeder-feeder" process in warm-frontal rainbands. *J. Atmos. Sci.*, **40**, 1185–1206.

Rutledge, S.A. and P.V. Hobbs, 1984: The mesoscale and microscale structure and organization of clouds and precipitation in midlatitude cyclones. Part XII: A diagnostic modeling study of precipitation development in narrow cold-frontal rainbands. *J. Atmos. Sci.*, **41**, 2949–2972.

Zhao, Q., F.H. Carr and G.B. Lesins, 1991: Improvement of precipitation forecasts by including cloud water and cloud ice into NMC's Eta model. *Proc., Nineth Conf. on Numerical Weather Prediction*, Denver, 14-18 October. Amer. Meteor. Soc., Boston, 50–53.

Appendix A : Description of Microphysical Option 5

I. Equation set

The equations used for water vapor q_v, cloud water q_c, rain water q_r, cloud ice q_i, snow q_s, and graupel q_g mixing ratios are the following:

$$\begin{aligned}\frac{\partial p^* q_v}{\partial t} &= -ADV(p^* q_v) + DIV(p^* q_v) + D(q_v) \\ &\quad + p^*(Prevp - Pidep - Psdep - Pgdep - Pidsn \\ &\quad - Pccnd)\end{aligned} \tag{1}$$

$$\begin{aligned}\frac{\partial p^* q_c}{\partial t} &= -ADV(p^* q_c) + DIV(p^* q_c) + D(q_c) \\ &\quad + p^*(-Pccnr - Pracw + Pccnd - Pifzc - Pispl - Ps.sacw \\ &\quad - Pg.sacw - Pgacw - Pi.iacw - Pg.iacw + Pimlt)\end{aligned} \tag{2}$$

$$\begin{aligned}\frac{\partial p^* q_r}{\partial t} &= -ADV(p^* q_r) + DIV(p^* q_r) \\ &\quad - Prprc + p^*(Pracw + Pccnr - Prevp - Pgfzr - Piacr \\ &\quad - Ps.sacr - Pg.sacr - Pgacr + Psmlt + Pgmlt)\end{aligned} \tag{3}$$

$$\begin{aligned}\frac{\partial p^* q_i}{\partial t} &= -ADV(p^* q_i) + DIV(p^* q_i) + D(q_i) \\ &\quad + p^*(Pidsn + Pifzc + Pispl + Pidep + Pi.iacw - Picng \\ &\quad - Praci - Psaci - Picns - Pimlt)\end{aligned} \tag{4}$$

$$\begin{aligned}\frac{\partial p^* q_s}{\partial t} &= -ADV(p^* q_s) + DIV(p^* q_s) \\ &\quad - Psprc + p^*(Psdep + Picns + Ps.sacw - Pscng + Psaci \\ &\quad + Ps.sacr - Pg.racs - Psmlt)\end{aligned} \tag{5}$$

$$\begin{aligned}\frac{\partial p^* q_g}{\partial t} &= -ADV(p^* q_g) + DIV(p^* q_g) \\ &\quad - Pgprc + p^*(Pgdep + Pscng + Pg.sacw + Pgacw + Pgacr \\ &\quad + Piacr + Praci + Pg.sacr + Pg.racs + Pgfzr \\ &\quad + Picng + Pg.iacw - Pgmlt)\end{aligned} \tag{6}$$

In addition to the prognostic equations for the mixing ratios, the prognostic equations for the number concentrations of cloud ice N_i, snow N_s, and graupel N_g are the following:

$$\begin{aligned}\frac{\partial p^* N_i}{\partial t} &= -ADV(p^* N_i) + DIV(p^* N_i) + D(N_i) \\ &\quad + p^*[-Nicng - Niag + Nifzc + \frac{\rho}{m_{io}}(Pidsn + Pispl) \\ &\quad - \frac{N_i}{q_i}(Pimlt + Praci + Psaci) - \frac{\rho Picns}{m_{so}}]\end{aligned} \tag{7}$$

$$\frac{\partial p^* N_s}{\partial t} = -ADV(p^* N_s) + DIV(p^* N_s) - Nsprc + p^*[-Ng.sacr - Nsag - Ngacs - Nscng + \frac{\rho Picns}{m_{so}} - \frac{N_s}{q_s}(Psmlt + Psdep)] \quad (8)$$

$$\frac{\partial p^* N_g}{\partial t} = -ADV(p^* N_g) + DIV(p^* N_g) - Ngprc + p^*[Nicng + \frac{N_i}{q_i}(Piacr + Praci) + Ng.sacr + Ngacs + Ngfzr - \frac{N_g}{q_g}(Pgmlt + Pgdep)] \quad (9)$$

Here p^* is the difference between the surface pressure and the pressure at the top, $\sigma = \frac{p-p_t}{p^*}$ with p the pressure and p_t the pressure at the top and D represents diffusion due to subgrid scale turbulence. The ADV and DIV terms in Eqs. (1)–(9) represent three-dimensional advection and divergence and are given by the following equations:

$$ADV(p^* f) = m^2 \left[\frac{\partial p^* uf/m}{\partial x} + \frac{\partial p^* vf/m}{\partial y}\right] + \frac{\partial p^* f\dot{\sigma}}{\partial \sigma} \quad (10)$$

$$DIV = m^2 \left[\frac{\partial p^* u/m}{\partial x} + \frac{\partial p^* v/m}{\partial y}\right] + \frac{\partial p^* \dot{\sigma}}{\partial \sigma}, \quad (11)$$

where m is the map-scale factor.

Unless otherwise specified source and sink terms along with constants in this microphysical scheme come from the following sources: Koenig [1971, (K)], Locatelli and Hobbs [1974 (LH)], Lin et al. [1983 (L)], Pruppacher and Klett [1980 (PK)], Ruteledge and Hobbs [1983 (RH) and 1984 (RH1)], Murakami [1990 (M)], Ikawa and Saito [1991 (IS)], and Grell et al. [1994 (GDS)]. Sources and sink terms for mass and number are designated by $Pqqqq$ and $Nqqqq$, respectively. Following IS, the subscripts are defined as follows: xdep for depositional growth of x, xmlt as melting of x, xprc for precipitation of x, xag for aggregation of x, xcny for conversion of x into y, xfzy for freezing of y to form x, xacy for the collection of y by x, x.yacz for generation of x as a result of collection of z by y, idsn for initiation of q_i, and ispl for the ice multiplication process (Hallet and Mossop 1974). For a brief description of each process see the end of this appendix.

In this bulk parameterization the size distribution function is expressed by an inverse exponential relationship of the form

$$N_x = \frac{N_{ox}}{\lambda_x} \quad (12)$$

where $\lambda_x = \left(\frac{\pi \rho_x N_x}{\rho q_x}\right)^{1/3}$ and $N_{ox} = N_x \left(\frac{\pi \rho_x N_x}{\rho q_x}\right)^{1/3}$ with ρ_x the density of a particular hydrometer and ρ the density of air. The change in the number concentration of the precipitable

hydrometer x due to precipitation is given as

$$Nxprc = -\frac{\partial V_{nf}\rho g N_x}{\partial \sigma} \tag{13}$$

where the number-weighted terminal velocity is defined as:

$$V_{nf} = \frac{a_x \Gamma(1+b_x)}{\lambda_x^{b_x}} \tag{14}$$

with $g = 9.8$ m s^{-2} is the gravitational acceleration and a_x and b_x being constants used in the fallspeed formula.

Likewise the change in the mixing ratio of the precipitable hydrometer x due to precipitation is given as

$$Pxprc = -\frac{\partial V_f \rho g q_x}{\partial \sigma} \tag{15}$$

where the mass-weighted mean terminal velocity defined as

$$V_f = \frac{a_x \Gamma(4+b_x)}{6\lambda_x^{b_x}} \tag{16}$$

The fall terms Eqs. (13) and (15) are calculated on split time-steps, $\Delta t'$, in the explicit moisture routine. This ensures that $V_f \Delta t'/\Delta z < 1$, which is required for numerical stability. The size of $\Delta t'$ is determined independently in each model column based on the maximum value of $V_f \Delta t/\Delta z$ in the column, where Δt is the model time step.

The saturated vapor pressure over water (in mb) is taken to be

$$e_{sw} = 6.112 \exp\left[17.67\left(\frac{T - T_0}{T - 29.65}\right)\right], \tag{17}$$

and for ice

$$e_{si} = 6.11 \exp\left(22.514 - \frac{6150}{T}\right) \tag{18}$$

with $T_0 = 237.15$ K is the temperature at the freezing point. The saturated water vapor mixing ratio with respect to water is then given by

$$q_{vsw} = \frac{0.622 e_{si}}{p - e_{si}} \tag{19a}$$

whereas the saturated water vapor mixing ratio with respect to ice is given by

$$q_{vsi} = \frac{0.622 e_{sw}}{p - e_{sw}} \tag{19b}$$

II. Production terms for q_i

A) Ice nucleation

If $q_v \geq q_{vsi}$, then Fletcher's (1962) curve is used for ice initiation which is given by the following formula:

$$n_c = 10^{-2}\exp[0.6(T_0 - T)] \tag{20}$$

Initiation occurs in the model when

$$Pidsn = \frac{m_{io}}{\rho}\frac{n_c - N_i}{2\Delta t} > 0 \tag{21}$$

where m_{io} is the mass of the smallest q_i.

B) Freezing of cloud droplets

Heterogeneous freezing of q_c to form q_i is based on work by Bigg (1953) and is parameterized as follows,

$$Pifrc = B'\{\exp[A'(T_0 - T)] - 1\}\frac{\rho q_c^2}{\rho_w N_c} \tag{22}$$

where $A' = 0.66$ K^{-1}, $B' = 100$ m^{-3}s^{-1}, $\rho_w = 1000$ kg m^{-3} is the density of water, and $N_c = 1 \times 10^8$ m^{-3} is the number concentration of cloud droplets.

C) homogeneous freezing of cloud droplets

When $T \leq 233.15$ K any q_c present immediately freezes to form q_i.

$$Pifzc = \frac{q_c}{2\Delta t} \qquad Nifzc = \frac{N_c}{2\Delta t} \tag{23}$$

D) Ice multiplication process

Ice multiplication is based on the work of Hallet and Mossop (1974) and is parameterized as follows:

$$Nispl = \rho \times 3.5 \times 10^8 f(T_c)(Ps.sacw + Pg.sacw) \tag{24}$$

where $f(T_c)$ is 0 for $T < 265$ K and $T > 270$ K, 1 for $T = 268$ K, and increases linearly between these two extremes for $T \geq 265$ K and $T \leq 270$ K.

The increase in mass of q_i associated with this process is given as

$$Pispl = \frac{Nispl \times m_{io}}{\rho} \tag{25}$$

E) Depositional growth of q_i

Depositional growth of q_i is given as

$$Pidep = \frac{q_v - q_{vsi}}{q_{vsw} - q_{vsi}} a_1 (m_i)^{a_2} N_i/\rho \tag{26}$$

where, a_1 and a_2 are temperature-dependent parameters from Koenig (1971), and $m_i = \frac{\rho q_i}{N_i}$ is the mass of a pristine ice crystal.

Note that the rates of depositional growth of q_i, q_s, and q_g along with $Pidsn$ are restricted to avoid overshooting into ice subsaturation in one time step.

F) Riming growth of q_i

$$Piacw = N_i \frac{\pi}{4}(D_i + D_c)^2 Eic|U_{di} - U_{dc}|q_c \tag{27}$$

where, $D_i = \left(\frac{6\rho q_i}{\pi \rho_i N_i}\right)^{1/3}$ is the diameter of q_i; $D_c = \left(\frac{6\rho q_c}{\pi \rho_w N_c}\right)^{1/3}$ the mean diameter of q_c; $U_{di} = 7 \times 10^2 D_i$; $U_{dc} = 3 \times 10^7 {D_c}^2$; and $Eic = 0.572 \times \log_{10}(\psi - 0.25) + 0.967$ with $\psi = D_c\left(\frac{\rho_w U_{di}}{\phi D_i}\right)^{1/2}$ and $\phi = 3.24 \times 10^{-4}$. Note, if $\phi < 0.25$, then $E_{ic} = 0$.

The portion of riming that goes into q_i production is

$$Pi.iacw = min(Piacw, Pidep) \tag{28}$$

with the amount $> Pidep$ going to form q_g $(Pg.iacw)$.

III. Production terms for q_s

A) Conversion of q_i to q_s

The time needed for an ice crystal to grow from m_i to m_{so} in $\Delta\tau$ via depositional and riming growth (IS Eqs. 27–29) is

$$\Delta\tau = \frac{N_i/\rho(m_{so} - m_i)}{Pidep + Pi.iacw};\ m_{so} = (4\pi/3)\rho_s r_{so}^3 \tag{29}$$

where r_{so}=0.75 $\times 10^{-4}$ m is the radius of the smallest snow particle.

Thus, the amount of q_i converted into q_s in unit time is given as $(m_i < 0.5 m_{so})$

$$CN_{is}^{dep+ac} = \frac{1}{\Delta\tau} q_i = \frac{m_i}{m_{so} - m_i}(Pidep + Pi.iacw) \tag{30a}$$

And for $m_i > 0.5 m_{so}$

$$CN_{is}^{dep+ac} = (Pidep + Pi.iacw) + \left(1 - \frac{0.5 m_{so}}{m_i}\right)\frac{q_i}{2\Delta t} \tag{30b}$$

Aggregation follows the parameterization developed by Murakami (1990, Eqs. 40–41) with the conversion rate from q_i to q_s being given by

$$Niag \equiv CN_{is}^{Ag} = \frac{q_i}{\Delta\tau_1} \tag{31}$$

where,

$$\Delta\tau_1 = -\frac{2}{C_1}\log\left(\frac{r_i}{r_{so}}\right)^3 \tag{32}$$

with $r_i = \left(\frac{6\rho q_i}{\pi\rho_i N_i}\right)$ the radius of q_i and

$$C_1 = \frac{\rho q_i a_i E_{ii} X}{\rho_i} \tag{33}$$

with $E_{ii} = 0.1$ the collection efficiency of amoung ice particles, and $X = 0.25$ the dispersion of the fall velocity of q_i.

Therefore the total conversion of q_i to q_s is

$$Picns = CN_{IS}^{dep+ac} + CN_{IS}^{Ag} \tag{34}$$

B) Aggregation amoung N_s

The decrease in N_s due to aggregation (Passarelli 1978) is parameterized as follows:

$$Nsag = \frac{-I(b_s)a_s E_{ss}}{4\times 720}\pi^{\frac{1-b_s}{3}}\rho^{\frac{2+b_s}{3}}\rho_s^{\frac{-2-b_s}{3}}q_s^{\frac{2+b_s}{3}}N_s^{\frac{4-b_s}{3}} \tag{35}$$

$E_{ss} = 0.1$ is the collection efficiency amoung snow particles, and $I(b_s) = 2566$, 1610, and 1108 for $b_s = 0.6$, 0.5, and 0.4.

C) Depositional growth and melting of q_s

Depositional growth of q_s (RH, Eq. A26) is given as

$$Psdep = \frac{4N_{os}(S_i-1)}{A'+B'}\left[\frac{0.65}{\lambda_s^2} + 0.44\left(\frac{a_s\rho}{\mu}\right)^{\frac{1}{2}}\frac{\Gamma(b_s/2+5/2)}{\lambda_s^{b_s/2+5/2}}\right] \tag{36}$$

where S_i is the saturation ratio over ice; $A' = \frac{L_s^2}{K_a R_w T^2}$ with L_s the latent heat of sublimation, K_a the thermal conductivity of air, R_w gas constant for q_v; and $B' = \frac{1}{\chi q_{vsi}}$ with χ the diffusivity of q_v in air.

Likewise melting of q_s (RH, Eq. A25) is given in a similiar form

$$Psmlt = -\frac{2\pi N_{os}}{L_f}K_a(T-T_0)\left[\frac{0.65}{\lambda_s^2} + 0.44\left(\frac{a_s\rho}{\mu}\right)^{\frac{1}{2}}\frac{\Gamma(b_s/2+5/2)}{\lambda_s^{b_s/2+5/2}}\right] \tag{37}$$

where L_f is the latent heat of fusion.

D) Collection of q_i by q_s

Collection of q_i by q_s (RH, Eq. A21) is parameterized as follows

$$Psaci = \frac{\pi a_s q_i E_{si} N_{os}}{4} \frac{\Gamma(b_s+3)}{\lambda_s^{b_s+3}} \tag{38}$$

where E_{si} is the collection efficiency for q_s collecting q_i.

IV Production terms for q_g

A) Conversion of q_i to q_g

The amount of q_i converted into q_g (IS, Eqs. 35–37) is given as

$$Picng = \frac{\rho Q_i}{\Delta m_{gi}} \max\left(\frac{Piacw - Pidep}{N_i}, 0\right) \tag{39}$$

where$\Delta m_{gi} = m_{go} - m_i$ with $m_{go} = 1.6 \times 10^{-10}$ kg the mass of the smallest graupel particle. The number of ice crystals to be converted into q_g is given as

$$Nicng = \rho\left(\frac{Picng + Pg.iacw}{m_{go}}\right) \tag{40}$$

B) Generation of q_g due to q_r and q_i collisions

The collection of q_i by q_r (RH1, Eq. A5) is given by

$$Praci = \frac{\pi}{4} q_i E_{ri} N_{or} \left[\frac{-0.267\Gamma(6)}{\lambda_r^6} + \frac{5.15\times10^3\Gamma(7)}{\lambda_r^7} - \frac{1.0225\times10^6\Gamma(8)}{\lambda_r^8} + \frac{7.55\times10^7\Gamma(9)}{\lambda_r^9}\right] \tag{41}$$

where $E_{ri} = 1$ is the collection efficiency for q_r collecting q_i.

The rate per time step which q_i collides with q_r (RH1, Eq. A7) can be expressed as

$$Piacr = N_i E_{ri} \frac{\pi^2}{24} \frac{\rho_l}{\rho} N_{or} \left[\frac{-0.267\Gamma(6)}{\lambda_r^6} + \frac{5.15\times10^3\Gamma(7)}{\lambda_r^7} - \frac{1.0225\times10^6\Gamma(8)}{\lambda_r^8} + \frac{7.55\times10^7\Gamma(9)}{\lambda_r^9}\right] \tag{42}$$

C) Conversion from q_s to q_g

The amount of rime on snow particles converted into q_g (IS, Eq. 46) is given as

$$Pg.sacw = \alpha 2\Delta t \frac{3\rho_o \pi N_{so} (\rho q_c)^2 E_{sc}^2 a_s^2 \Gamma(2b_s+2)}{8\rho(\rho_g - \rho_s)\lambda_s^{2b_s+2}} \tag{43}$$

where $\alpha = 4$ is a tuning parameter, $\rho_o = 1$ kg m^{-3} is the basic state density, and $E_{sc} = 1$ is the collection efficiency for q_s collecting q_c.

The amount of q_s converted into q_g as embryo (Murakami, Eq. 43) is given as

$$Pscng = \max\left(\frac{\rho_s}{\rho_g - \rho_s} Pg.sacw, 0\right) \tag{44}$$

The amount of riming consumed for the growth of q_s itself is

$$Ps.sacw = Psacw - Pg.sacw \tag{45}$$

where

$$Psacw = \frac{\pi a_s q_c E_{sc} N_{os}}{4} \frac{\Gamma(b_s + 3)}{\lambda_s^{b_s+3}} \tag{46}$$

is from RH Eq. 22.

D) Collisions between q_r and q_s

Collection of q_r by q_s (IS, Eq. 57) is given as

$$Psacr = \pi^2 E_{rs} \sqrt{(\alpha V_r - \beta V_s)^2 + \gamma V_r V_s} \frac{\rho_w}{\rho} N_{ro} N_{so} \left(\frac{5}{\lambda_r^6 \lambda_s} + \frac{2}{\lambda_r^5 \lambda_s^2} + \frac{0.5}{\lambda_r^4 \lambda_s^3}\right) \tag{47}$$

where $\alpha = 1.2$, $\beta = 0.95$, $\gamma = 0.08$, and $E_{rs} = 1$ is the collection efficiency between q_s and q_r.

Likewise the collection of q_s by q_r (IS, Eq. 58) is given as

$$Pracs = \pi^2 E_{rs} \sqrt{(\alpha V_r - \beta V_s)^2 + \gamma V_r V_s} \frac{\rho_s}{\rho} N_{ro} N_{so} \left(\frac{5}{\lambda_s^6 \lambda_r} + \frac{2}{\lambda_s^5 \lambda_r^2} + \frac{0.5}{\lambda_s^4 \lambda_r^3}\right) \tag{48}$$

The number of collisions between q_s and q_r (IS, Eq. 60) is given as

$$Nsacr = Nracs = \frac{\pi}{2} E_{rs} \sqrt{\alpha (V_{nr} - V_{ns})^2 + \beta V_{nr} V_{ns}} N_{ro} N_{so} \left(\frac{1}{\lambda_r^3 \lambda_s} + \frac{1}{\lambda_r^2 \lambda_s^2} + \frac{1}{\lambda_r \lambda_s^3}\right) \tag{49}$$

where $\alpha = 1.7$, and $\beta = 0.3$.

The portion of the collected q_r by q_s consumed for production of q_g (IS, Eq. 63) in mass is

$$Pg.racs = (1 - \alpha_{rs}) Pracs \tag{50}$$

where

$$\alpha_{rs} = \frac{\rho_s^2 \left[\frac{4}{\lambda_s}\right]^6}{\rho_s^2 \left[\frac{4}{\lambda_s}\right]^6 + \rho_w^2 \left[\frac{4}{\lambda_r}\right]^6} \tag{51}$$

The portion of the collected q_r by q_s consumed for production of q_g (IS, Eq. 63) is

$$Pg.sacr = (1 - \alpha_{rs}) Psacr \tag{52}$$

The portion of the collected q_r by q_s consumed for the production of q_s (IS, Eq. 64) is

$$Ps.sacr = \alpha_{rs} Psacr \tag{53}$$

N_g generation by collisions of q_s and q_r (IS, Eq. 65) is expressed as

$$Ng.racs = (1 - \alpha_{rs}) Nracs = Ng.sacr \tag{54}$$

Note, similar approximations are used in deriving the rates involving collisions between graupel and rain ($Pgacr$).

E) Q_g generation via freezing of q_r

Freezing of q_r to produce q_g is based on Bigg's (1953) work and is given as

$$Ngfzr = B'' \pi N_{or} \lambda_r^{-4} \tag{55}$$

where $B'' = B'(\exp(A(T_0 - T)) - 1)$, $B' = 100$ m^{-3} s^{-1} and $A' = 0.66$ (K^{-1}). The increase in mass is given by

$$Pgfzr = 20\pi^2 B' N_{or} \frac{\rho_w}{\rho} (\exp(A(T_0 - T)) - 1) \gamma_r^{-7} \tag{56}$$

F) Depositional growth and melting of q_g

Depositional growth of q_g (RH1, Eq. A17) is given as

$$Pgdep = \frac{2\pi N_{og}(S_i - 1)}{A' + B'} \left[\frac{0.78}{\lambda_g^2} + 0.31 \left(\frac{a_g \rho}{\mu} \right)^{\frac{1}{2}} \frac{\Gamma(b_g/2 + 5/2)}{\lambda_g^{b_g/2+5/2}} \right] \tag{57}$$

Melting of q_g (RH1, Eq. A18) is formulated as

$$Pgmlt = \frac{-2\pi}{L_f} K_a (T - T_0) N_{og} \left[\frac{0.78}{\lambda_g^2} + 0.31 \left(\frac{a_g \rho}{\mu} \right)^{\frac{1}{2}} \frac{\Gamma(b_g/2 + 5/2)}{\lambda_g^{b_g/2+5/2}} \right] \tag{58}$$

In addition, enhanced melting of q_g due to the collection of q_c by q_g and q_r by q_g (RH1, Eqs. A21–22) is included in the $Pgmlt$ term.

G) Production of q_g by collection of q_c by q_g

$$Pgacw = \frac{\pi a_g q_c E_{gc} N_{og}}{4} \frac{\Gamma(b_g + 3)}{\lambda_g^{b_g+3}} \tag{59}$$

where $E_{gc} = 1$ is the collection efficiency for q_g collecting q_c.

V. Production terms for q_r

A) Conversion from q_c into q_r

The collision and coalescence of cloud droplets to form raindrops has been parameterized by use of the Kessler parameterization

$$Pccnr = a\,H(Q_c - Q_{co}) \tag{60}$$

where $a = 1 \times 10^{-3}$ s^{-1} is a time constant, H is a Heaviside function, and $Q_{co} = 0.5 \times 10^{-3}$ is a cuttoff value.

B) Collection of q_c by q_r

Collection of q_c by q_r (GDS, Eq. 5.3.1.1.8) is given as

$$Pracw = \frac{\pi}{4} a_r \rho q_c E_{rc} N_{or} \frac{\Gamma(3+b_r)}{\lambda^{3+b_r}} \tag{61}$$

with $E_{rc} = 1$ is the collection efficiency between q_c and q_r.

c) Sublimation/evaporation of rainwater

Evaporation of q_r is parameterized (RH, Eq. 12) by

$$Prevp = \frac{2\pi N_{or}(S_w - 1)}{A' + B'} \left[\frac{0.78}{\lambda_r^2} + 0.31 \left(\frac{a_r \rho}{\mu} \right)^{\frac{1}{2}} \frac{\Gamma(b_r/2 + 5/2)}{\lambda_r^{b_r/2+5/2}} \right] \tag{62}$$

with L_v being substituted for L_s in Eq. 36.

VI Production terms for q_c

A) conversion from q_v into q_c

Pccnd, the condensation is determined as follows. Temperature, water vapor mixing ratio and cloud water are forecast first: these preliminary forecast values are designated by T^*, q_v^* and q_c^*. We define

$$\delta M = q_v^* - q_{vsw}^*,$$

where q_{vsw}^* is the saturated mixing ratio at temperature T^*,

(1) if $\delta M > 0$ (supersaturation),

$$Pccnd = \frac{r_1 \delta M}{\Delta t}, \tag{63}$$

where

$$r_1 = \frac{1}{1 + \frac{L_v^2 q_{vsw}^*}{R_v c_{pm} T^{*2}}},$$

(2) if $\delta M < 0$ and $q_c > 0$ (evaporation),

$$Pccnd = -\min\left[-\frac{r_1 \delta M}{\Delta t}, \frac{q_c^*}{\Delta t}\right], \tag{64}$$

(3) if $\delta M < 0$ and $q_c = 0$,

$$Pccnd = 0. \tag{65}$$

The $Pccnd$ term is computed diagnostically so no iteration is needed.

B) Melting of q_i to form q_c

If q_i is present at $T > 273K$ it melts instantly to form q_c.

$$Pimlt = \frac{q_i}{2\Delta t} \tag{66}$$

Thus, the latent heating due to explicit moisture only is as follows

$$\begin{aligned}\dot{\theta} = & -L_v(Prevp - Pccnd) + L_s(Pidep + Pidsn + Psdep + Pgdep) \\ & + L_f(Pi.iacw + Pg.iacw + Ps.sacw + Pg.sacw + Pgacw + Piacr \\ & + Pifzc + Pgfzr + Psacr + Pgacr - Pimlt - Psmlt - Pgmlt)\end{aligned} \tag{67}$$

VII. Numerical Artifacts

Occasionally, the sum total of the source and sink terms in Eqs. (1–9) becomes so large that a given microphysical variable can become negative. To circumvent this problem the terms are adjusted by dividing each microphysical rate term by the sum total of the rates.

Even with this adjustment procedure in place, due to the implementation of a leap-frog time step in MM5 negative values of the microphysical variables can occur. At present, the negative values are simply set equal to zero.

Another common problem is that imbalances between mass and number can give rise to erroneous results. To prevent this the number concentrations are bound by the following constraints:

for q_i

$$\frac{0.5 \times \rho q_i}{0.8 m_{so}} < N_i < \frac{100 \rho q_i}{m_{io}} \tag{68}$$

for q_s

$$\left(\frac{N_{so}}{1000}\right)^{3/4} \left(\frac{\rho q_s}{\rho_s \pi}\right)^{1/4} < N_s < (1000 N_{os})^{3/4} \left(\frac{\rho q_s}{\rho_s \pi}\right)^{1/4} \tag{69}$$

and for q_g

$$10^{-7} \times \left(\frac{\rho q_g}{m_{go}}\right) < N_g < 100 \times \left(\frac{\rho q_g}{m_{go}}\right) \tag{70}$$

Sekhon and Srivastava (1970) determined that better comparison against observed snow distributions can be obtained in theoretical studies if the slope intercept value for the size distribution is expressed as

$$N_{0s}(m^{-4}) = 1.05R^{-0.94} \tag{5.3.1.2.3}$$

where, N_{0s} is the slope intercept and R (m s^{-1}) is the snow fall rate. Thus a variable intercept parameter replaces the constant N_{0s} used in the simple ice scheme.

This can be expressed in terms of snow mixing ratio, q_S, as

$$N_{0s} = \left\{ 1.05 \left[\frac{1}{\rho q_S \alpha} \left(\frac{\pi \rho_S}{\rho q_S} \right)^{\frac{b}{4}} \right]^{0.94} \right\}^{\frac{4}{0.94b+4}} \tag{5.3.1.2.4}$$

where, $\alpha^{-1} = \frac{6\rho_w}{a\Gamma(4+b)}$.